Secreted Phosphoprotein 1 Is a Determinant of Lung Function Development in Mice

Koustav Ganguly^{1,4}, Timothy M. Martin¹, Vincent J. Concel¹, Swapna Upadhyay^{1,5}, Kiflai Bein¹, Kelly A. Brant¹, Leema George⁴, Ankita Mitra⁴, Tania A. Thimraj⁴, James P. Fabisiak¹, Louis J. Vuga^{2,3}, Cheryl Fattman¹, Naftali Kaminski^{2,3,6}, Holger Schulz⁷, and George D. Leikauf¹

¹Department of Environmental and Occupational Health, Graduate School of Public Health, ²Department of Medicine, and ³Simmons Center for Interstitial Lung Disease, Department of Medicine, University of Pittsburgh, Pittsburgh, Pennsylvania; ⁴SRM Research Institute, SRM University, Chennai, Tamil Nadu, India; ⁵Department of Biotechnology, Indian Institute of Technology Madras, Chennai, Tamil Nadu, India; ⁶Pulmonary, Critical Care and Sleep Medicine, Department of Medicine, Yale School of Medicine, New Haven, Connecticut; and ⁷Institute of Epidemiology I, Helmholtz Zentrum Munich, German Research Center for Environmental Health, Neuherberg, Munich, Germany

Abstract

Secreted phosphoprotein 1 (*Spp1*) is located within quantitative trait loci associated with lung function that was previously identified by contrasting C3H/HeJ and JF1/Msf mouse strains that have extremely divergent lung function. JF1/Msf mice with diminished lung function had reduced lung SPP1 transcript and protein during the peak stage of alveologenesis (postnatal day [P]14–P28) as compared with C3H/HeJ mice. In addition to a previously identified genetic variant that altered runt-related transcription factor 2 (RUNX2) binding in the *Spp1* promoter, we identified another promoter variant in a putative RUNX2 binding site that increased the DNA protein binding. SPP1 induced dose-dependent mouse lung epithelial-15 cell proliferation. $Spp1^{(--/-)}$ mice have decreased specific total lung capacity/body weight, higher specific compliance, and increased mean airspace chord length (L_m) compared with $Spp1^{(+/+)}$ mice. Microarray

analysis revealed enriched gene ontogeny categories, with numerous genes associated with lung development and/or respiratory disease. Insulin-like growth factor 1, Hedgehog-interacting protein, wingless-related mouse mammary tumor virus integration site 5A, and NOTCH1 transcripts decreased in the lung of P14 $Spp1^{(-/-)}$ mice as determined by quantitative RT-PCR analysis. SPP1 promotes pneumocyte growth, and mice lacking SPP1 have smaller, more compliant lungs with enlarged airspace (i.e., increased L_m). Microarray analysis suggests a dysregulation of key lung developmental transcripts in gene-targeted $Spp1^{(-/-)}$ mice, particularly during the peak phase of alveologenesis. In addition to its known roles in lung disease, this study supports SPP1 as a determinant of lung development in mice.

Keywords: osteopontin; chronic obstructive pulmonary disease; asthma; emphysema; pulmonary fibrosis

Chronic lung diseases are leading causes of death worldwide (1). Impaired lung development is associated with lower basal pulmonary function and with defective repair and remodeling processes after lung injury, thereby predisposing individuals to chronic lung disease (2–7). Recently, the

molecular pathways of lung development have been described (8, 9), and genes associated with lung function have been identified by genome-wide association studies (GWAS) (10–14). However, genetic variants in significant loci explained only a modest portion of the variance for FEV₁/

FVC (15, 16). Thus, much of the heritability remains unexplained by individual variants identified in GWAS, which is common with complex phenotypes (17, 18). In addition, the functional consequence of these genes and the downstream effectors of lung function have not been fully explored.

(Received in original form November 4, 2013; accepted in final form April 27, 2014)

This study was supported by the National Institutes of Health grants ES015675, HL077763, and HL085655 (G.D.L.); HL084932 and HL095397 (N.K.); and DST SERB: SB/SO/AS-026/2013 (K.G.).

Author Contributions: K.G., H.S., N.K., and G.D.L. conceived the project and designed the experiments. K.G., T.M.M., V.J.C., S.U., K.B., K.A.B., and L.J.V. performed the experiments. K.G., H.S., N.K., G.D.L., J.P.F., L.G., A.M., T.A.T., and C.F. analyzed the data. K.G., L.G., H.S., and G.D.L. wrote the manuscript.

Correspondence and requests for reprints should be addressed to Koustav Ganguly, Ph.D., Department of Environmental and Occupational Health, Graduate School of Public Health, University of Pittsburgh, 100 Technology Drive, Suite 350, Pittsburgh, PA 15219-3130. E-mail: kog8@pitt.edu; or to George D. Leikauf, Ph.D., Department of Environmental and Occupational Health, Graduate School of Public Health, University of Pittsburgh, 100 Technology Drive, Suite 350, Pittsburgh, PA 15219-3130. E-mail: gleikauf@pitt.edu

This article has an online supplement, which is accessible from this issue's table of contents at www.atsjournals.org

Am J Respir Cell Mol Biol Vol 51, Iss 5, pp 637–651, Nov 2014 Copyright © 2014 by the American Thoracic Society Originally Published in Press as DOI: 10.1165/rcmb.2013-0471OC on May 9, 2014 Internet address: www.atsjournals.org

Clinical Relevance

Inappropriate lung development is a risk factor for lower basal pulmonary function as well as defective repair and remodeling processes after lung injury, thereby predisposing individuals to asthma, pulmonary fibrosis, and chronic obstructive pulmonary diseases (COPD). This study examines the role of secreted phosphoprotein 1 (SPP1), a protein previously associated with pulmonary fibrosis and COPD, in lung development in mice. A mouse strain with decreased lung function has decreased lung SPP1 during postnatal alveologenesis. Mice have a genetic variant in the Spp1 promoter that is near a similar transcription factor binding site that is variant in humans. Spp1-deficent mice have smaller alveoli and decreased lung function.

To further address the genetics of lung development and function, we used a diverse panel of inbred mice (19), a model organism with an extensive genetic architecture. We previously identified several quantitative trait loci (QTL) for lung function in mice by contrasting two strains (C3H/HeJ versus JF1/Msf) with extremely divergent pulmonary function (e.g., total lung capacity [TLC] of C3H/HeJ = 1,443 \pm 30 μ l and JF1/Msf = 874 \pm 17 μ l) (19, 20). We had previously identified candidate genes located in QTL on various regions of mouse chromosome 5, including superoxide dismutase 3, extracellular (Sod3) (21, 22), and c-Kit oncogene (Kit) (23), as determinants of dead space volume and lung compliance (C_L), respectively. In children, we found that SOD3 singlenucleotide polymorphisms (SNPs) were associated with decreased FEV1 and maximal expiratory flow at 25% volume (22). In adults, SOD3 SNPs have been associated with lower lung function (24, 25) and increased risk of developing chronic obstructive pulmonary disease (COPD) (26). These findings support the rapid identification of candidate genes in mice that can later be tested in human populations.

In this study we sought to determine whether secreted phosphoprotein 1 (*Spp1*, a.k.a. osteopontin) is a functional candidate gene for lung development in mice. *Spp1* is

located within another QTL associated with lung function on mouse chromosome 5 bounded by markers D5Mit20 to D5Mit403 (97.8-106.2 Mbp) (20, 21), which is syntenic to human chromosome 4 (81.8-90.2 Mbp). SPP1 has been associated with chronic lung diseases, including pulmonary fibrosis (27) and COPD (28). An approximately 44 kD glycosylated phosphoprotein, SPP1, is commonly found in adhesive bone matrix protein. It is also recognized as a key cytokine involved in immune cell recruitment and type-1 (Th1) cytokine expression at sites of inflammation (29, 30) and as a mediator of tissue repair and remodeling (31, 32). Past studies on SPP1 focused mainly on its association with bone metabolism, inflammation, and cancer; however, the role of SPP1 in lung development is unknown.

In this study we examined lung SPP1 expression in mice and found strain-specific differences during development. Previously, Shen and Christakos (33) reported that the mouse Spp1 promoter contained functional runt-related transcription factor 2 (RUNX2) (-136 to -130 bp from the)transcription start site) and vitamin D response element (-757 to -743)binding sites that cooperatively regulate transcriptional activation by 1,25dihydroxyvitamin D₃ [1,25(OH) D₃]. In cells transfected with hes family bHLH transcription factor 1 (a.k.a. hairy and enhancer of split 1 [HES1]), basal and 1,25(OH) D₃-induced SPP1 transcripts increased, indicating involvement of the NOTCH1 pathway. Subsequently, Sowa and colleagues (34) PCR amplified and sequenced the mouse *Spp1* promoter in the C3H/HeJ and compared this sequence with the promoter of the reference C57BL/6J strain. One variant, a 13-bp insertion (rs234069704) at position -130 (5'-TTTTTTTTTTA-3'), was located at the 3' end of the RUNX2 binding site. This insertion increased transcriptional responsiveness to RUNX2 in the C3H/HeJ promoter as compared with that of the C57BL/6J promoter. Based on these studies, we further examined Spp1 promoter polymorphisms in mice.

Materials and Methods

Detailed methods are provided in the online supplement. Briefly, studies were approved by the Bavarian Animal Research Authority and by the IACUC of the University of Pittsburgh. Mice (C3H/HeJ, JF1/Msf, *Spp1*^(-/-)

 $[B6.129S6(Cg)-Spp1^{tm1Blh}/J]$, and $Spp1^{(+/+)}$ [C57BL/6J]) were purchased from Jackson Laboratory (Bar Harbor, ME). Quantitative RT-PCR (qRT-PCR) was used to determine lung SPP1 transcripts using the $2^{-\Delta\Delta CT}$ method normalized to actin, β (ACTB) as described previously (21). ELISA was used to determine lung SPP1 protein levels. Mouse lung epithelial (MLE)-15 cells are an immortalized cell line obtained from transgenic mice containing the simian virus 40 large T antigen under the transcriptional control of the human surfactant protein C promoter (35, 36). To measure the effect of SPP1 on cell proliferation, subconfluent MLE15 cells were serum deprived for 24 hours, 0 (control) or 1 to 4 µg/ml SPP1 was added to the culture medium, and growth was assessed at 48 hours using an alamarBlue (Life Technologies, Grand Island, NY) cell viability assay. To assess the effects of SNPs on the binding of nuclear protein, PCR amplification of the Spp1 promoter region was performed using genomic DNA from C3H/HeJ and JF1/Msf mice and sequenced in forward and reverse directions (Sequiserve, Vaterstetten, Germany). Two of the identified SNPs were used for an electrophoretic mobility shift assay (EMSA) performed using nuclear protein extracts from MLE15 cells. Doublestranded 25-mer oligonucleotides were prepared by annealing complementary synthetic oligonucleotides corresponding to the Spp1 promoter region containing G/T rs264140167 or A/G rs47003578 alleles. Lung function was measured in 27 strains of inbred mice (females, 13-17 wk; n = 252) and $Spp1^{(-/-)}$ and strain-, sex-, and agematched control $Spp1^{(+/+)}$ mice as described (19, 20, 37). To assess lung morphology, mean airspace chord length (L_m) was measured from images to estimate the alveolar size of $Spp1^{(-/-)}$ mice and compared with strain-, sex-, and agematched $Spp1^{(+/+)}$ as described (22). For immnunohistochemical localization, Spp1^(+/+) lung sections were stained using a goat anti-mouse SPP1 antibody (AF-808; R&D Systems, Inc., Pittsburgh, PA) and biotinylated horse anti-goat secondary antibody (1:200 dilution) (Vector Laboratories, Inc., Burlingame, CA). Lung transcript levels were measured by microarray (Whole Mouse Genome Kit 4 × 44K; Agilent Technologies, Santa Clara, CA) comparing postnatal day (P)14 $Spp1^{(-/-)}$ with P14 $Spp1^{(+/+)}$ and P28 $Spp1^{(-/-)}$ with P28 $Spp1^{(+/+)}$ mice. P14 and P28 were

chosen based on reduced SPP1 transcript expression pattern in JF1/Msf lungs compared with C3H/HeJ during peak phase of alveologenesis (P14) and completion of alveologenesis (P28). In addition, insulinlike growth factor 1 (IGF1), winglessrelated mouse mammary tumor virus integration site 5A (WNT5A), Hedgehoginteracting protein (HHIP), notch 1 (NOTCH1), CD44 antigen (CD44) transcripts were assessed by qRT-PCR using lung RNA from P14 or P28 Spp1^(-/-) or from P14 or P28 $Spp1^{(+/+)}$ mice. Data are presented as mean values of nobservations \pm the standard error (SE). Group comparisons were performed using ANOVA and all pairwise comparisons procedure (Holm-Sidak method) (Plot 11.0 software; Sigma). Significant differences in transcript levels for the microarray data were analyzed using ANOVA (Partek Genomics Suite; Partek, St. Louis, MO).

Results

Lung SPP1 Transcript and Protein Expression

Lung SPP1 transcripts decreased in JF1/Msf mice as compared with C3H/HeJ mice during various stages of postnatal lung development between P14 and P70 (Figure 1A). At P7, lung SPP1 transcripts in JF1/Msf mice were not significantly different than in C3H/HeJ mice. However, from P14 onward, lung SPP1 transcripts decreased in JF1/Msf as compared with C3H/HeJ mice. At P28, lung SPP1 protein

decreased in JF1/Msf as compared with C3H/HeJ mice (Figure 1B).

Spp1 Promoter Analysis

The mouse *Spp1* promoter contained a functional RUNX2 binding site (-136 to -130) (33). A 13-bp insertion (rs234069704) at position -130 (5'-TTTTTTTTTTTA-3') was located at the 3' end of this binding site that increases transcriptional responsiveness to RUNX2 in the C3H/HeJ promoter as compared with that of the C57BL/6J promoter (34). To further analyze the mouse Spp1 promoter, approximately 700-bp fragments 5' from the transcription start site of the mouse Spp1 gene were PCR amplified using the JF1/Msf or C3H/HeJ DNA as a template and sequenced. These sequences were aligned to the reference sequence (obtained from C57BL/6J) (see Figure E1 in the online supplement), and six genetic variants (four single SNPs and two insertions) were identified that differed between IF1/Msf and C3H/HeJ mice (see Table E1). Like the reference C57BL/6J, the JF1/Msf promoter lacks the 13-bp insertion rs234069704. The variation in sequence was then analyzed using Matinspector (38) to identify which of the other four genetic variants could alter putative transcriptional binding sites. Two of the identified SNPs at position -158 (rs264140167) and -198 (rs47003578) could alter putative binding

Sequence information of these two SNPs was used to generate 25-mer biotinylated oligonucleotide probes for

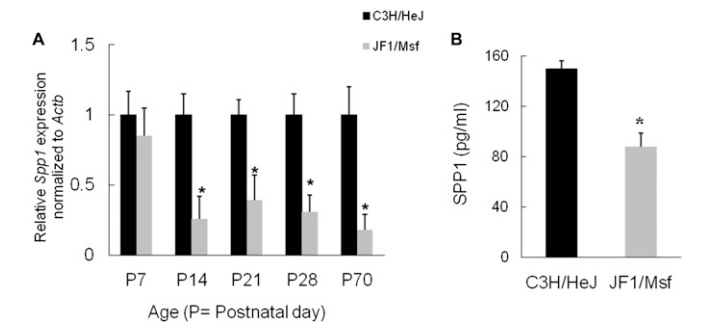


Figure 1. Lung secreted phosphoprotein 1 (SPP1) transcript and protein decreased in JF1/Msf mice as compared with C3H/HeJ mice. (*A*) During postnatal lung development (i.e., postnatal day [P] 7–P70), lung SPP1 transcript decreased in JF1/Msf mice as compared with C3H/HeJ mice. Previously we determined that JF1/Msf mice have diminished lung function as compared with C3H/HeJ mice (20, 21). Reduced transcripts (\sim 4-fold) were first noted at P14, which is the peak stage of alveologenesis. (*B*) Lung SPP1 protein decreased 1.7-fold in P28 JF1/Msf mice as compared with P28 C3H/HeJ mice. Values are mean \pm SE (n=5 mice/strain). Statistical significance (*P < 0.05) was determined by ANOVA and by the all pairwise comparisons procedure (Holm-Sidak method).

EMSA of nuclear protein extract prepared from MLE-15 cells. SNP rs264140167 (-158 nucleotides from the transcription)start site) in the Spp1 promoter region alters the nuclear protein-target DNA binding capacity. The 25-mer probes (-144to -168 bp) containing C3H/HeJ T allele in the middle of the biotinylated oligonucleotide increased the DNA protein binding (i.e., the C3H/HeJ T allele formed slow migrating complexes and enhanced the intensity of a faster migrating complex compared with the JF1/Msf G allele) (Figure 2). The C3H/HeJ T allele forms an additional putative RUNX2 binding site not present in the JF1/Msf G allele. No difference in protein binding was noted in the EMSA when probes were generated from the rs47003578 SNP (JF1/Msf G allele versus C3H/HeJ A allele), which is located -198 nucleotides from the transcription start site (Figure E2).

We examined the lung functions of 36 inbred strains of mice to determine the possible functional consequence of rs47003578 SNP (JF1/Msf G allele versus C3H/HeJ A allele). This includes nine strains that had been previously phenotyped (19, 20) and 27 additional mouse strains (Table 1). Mice with the JF1/Msf allele had decreased TLC (G allele = 1,144 ± 13 versus T allele = 1,205 \pm 25 μ l; n = 345mice), decreased specific TLC/body weight (G allele = 54 ± 1 versus T allele = 57 ± 1 μ l/g; n = 369 mice), and increased specific compliance (C_I/TLC) (G allele = 58 \pm 1 versus T allele = $54 \pm 1 \mu l/cm H_2O/ml$; n =354 mice) (n = 7-15 mice/strain, 12-14 wk). These differences are \sim 11, 17, and 21%, respectively, of the phenotypic difference we have previously observed in the extremely divergent mouse strains (19, 20). Body weight (G allele = 22.5 ± 0.4 versus T allele = 22.6 \pm 0.6 g; n = 382 mice) and other lung function measurements (e.g., dead space volume) were not statistically different between genotypes.

SPP1 Induces Mouse Pneumocyte Growth

Considering that lung SPP1 transcripts and protein decreased in JF1/Msf mice during the peak stage of alveologenesis, we investigated whether SPP1 protein could stimulate the growth of MLE cells. MLE-15 cell proliferation increased 48 hours after treatment with 2 and 4 μ g/ml SPP1 (Figure E3).

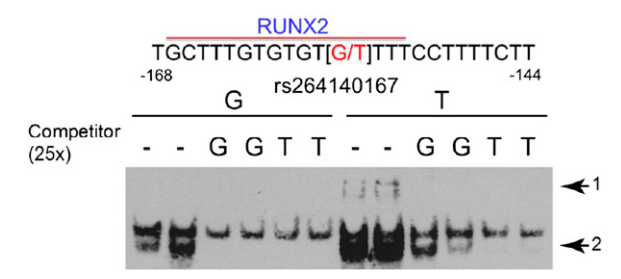


Figure 2. Genetic variant in secreted phosphoprotein 1 (Spp1) promoter alters nuclear protein binding capacity. Electrophoretic mobility shift assay of nuclear protein extract prepared from mouse lung epithelial cells (MLE15) and 25-mer probes (-144 to -168 bp from the start site). The single nucleotide polymorphism rs264140167 (-158 nucleotides from the transcription start site) in the Spp1 promoter region was used to generate 25-mer probes containing the C3H/HeJ T allele or the JF1/Msf G allele in the middle of the biotinylated oligonucleotide. The C3H/HeJ T allele increased the DNA protein binding to form slow migrating complexes (arrow 1) and enhanced the intensity of a faster migrating complex (arrow 2) compared with the JF1/Msf G allele. The C3H/HeJ T allele forms an additional putative runt-related transcription factor 2 (RUNX2) binding site not present in the JF1/Msf G allele.

Lung Function of Spp1^(-/-) Mice

Analysis of lung function revealed that $Spp1^{(-/-)}$ had decreased TLC ($Spp1^{(-/-)}$ = 1,034 \pm 25 versus $Spp1^{(+/+)}$ = 1,220 \pm 22 μ l), decreased specific TLC/body weight

 $(Spp1^{(-/-)} = 48 \pm 1 \text{ versus } Spp1^{(+/+)} = 58 \pm 1 \text{ µl/g}), \text{ and increased specific } C_L$ $(Spp1^{(-/-)} = 54 \pm 1 \text{ versus } Spp1^{(+/+)} = 47 \pm 1 \text{ µl/cm } H_2O/\text{ml}) (n = 8 \text{ mice/strain}, 12-14 \text{ wk}) (Figure 3). These differences$ are approximately 33, 38, and 16%, respectively, of the phenotypic difference we have previously observed in the extremely divergent mouse strains (20). Other lung function measurements (including dead space volume and diffusion capacity/TLC) and BW $(Spp1^{(-/-)} = 21.5 \pm 0.9 \text{ versus } Spp1^{(+/+)} = 21.0 \pm 0.8 \text{ g})$ were not statistically different between $Spp1^{(-/-)}$ and $Spp1^{(+/+)}$ mice.

Lung Morphometry and SPP1 Immunohistochemical Location

Increased L_m indicates decreased alveolar surface area. The mean chord length in $Spp1^{(-/-)}$ increased as compared with $Spp1^{(+/+)}$ mice (Figure 4). This was detected in P28 mice when lung development is just completed and is indicative of impaired alveologenesis. Immunohistological analysis localized SPP1 protein to the bronchial epithelium, alveolar macrophage, and weakly to the alveolar type II cell in adult $Spp1^{(+/+)}$ mice (Figure E4).

Table 1. Lung Function Values of 27 Inbred Mouse Strains (female; N = 252 mice)

Strain	Mice Phenotyped/ Strain	Age* (<i>wk</i>)	BW* (g)	BW SE	TLC* (μ/)	TLC SE	TLC/BW* (μ//g)	TLC/BW SE	sC _L * (<i>ml</i>)	sC _L SE	V _D * (μ <i>l</i>)	V _D SE
AKR/J	.8	16.0	30.6	1.2	1,176	32	40.9	1.5	49.8	2.7	231	4
BALB/cJ	10	13.9	22.7	0.8	1,277	17	60.2	2.5	63.9	3.0	233	2
BPL/1J	10	14.2	16.9	0.4	1,046	16	66.5	1.7	72.4	3.2	230	2
BTBR T ⁺ tf/	8	13.9	31.9	0.6	1,409	26	46.5	1.6	58.2	1.7	251	3
BUB/BnJ	10	14.1	25.6	0.6	1,097	38	45.1	1.2	58.0	3.2	225	2
C3HeB/FeJ	10	14.4	25.7	0.9	1,480	33	61.6	2.3	72.9	4.0	232	3
C57BL/10J	10	14.3	20.7	0.4	1,034	11	52.7	1.0	51.2	0.7	233	4
C57BLKS/J	10	14.3	21.7	0.6	1,131	24	54.8	1.2	55.6	2.7	233	5
C57BR/cdJ	9	13.9	24.0	1.1	1,116	28	49.1	2.2	54.4	3.0	221	4
C57L/J	9	15.8	22.7	0.3	1,209	26	55.8	0.9	55.0	1.3	244	2
C58/J	10	14.7	19.8	0.5	1,002	20	53.7	0.9	53.2	1.1	215	2
CBA/J	10	15.3	28.6	0.5	1,177	17	43.4	0.9	59.8	3.4	242	1
DBA/1J	8	16.4	20.9	0.5	971	14	49.2	1.4	52.7	2.1	231	5
DBA/2J	8 7	15.4	24.2	8.0	1,054	17	45.8	1.7	58.0	1.3	232	3
KK/HIJ		13.9	35.0	1.3	1,304	29	39.6	1.5	47.0	1.9	246	2
LP/J	8	14.3	18.9	0.5	1,074	29	59.6	1.7	61.6	2.9	241	4
MRL/MpJ	10	13.9	35.5	1.3	1,519	42	45.0	1.1	56.3	3.7	251	3
NOD/ShiLtJ	8	15.1	21.9	0.6	1,012	25	48.8	1.6	60.7	2.4	222	2
NON/ShiLtJ	8	14.3	31.3	0.9	1,426	26	48.4	1.6	75.1	3.2	255	2
NZL/LtJ	9	14.4	36.3	1.9	1,409	34	41.9	2.2	59.6	2.5	230	2
NZW/LacJ	8	14.3	27.4	0.8	1,218	26	46.8	0.7	75.9	5.5	250	4
PL/J	10	14.1	20.5	0.7	956	13	49.7	1.2	49.0	1.2	210	3 5
PWD/PhJ	14	15.2	15.8	0.3	967	21	64.8	1.5	33.4	1.2	202	5
RIIIS/J	10	14.2	17.8	0.4	995	25	59.2	2.0	55.1	3.3	221	3
SJL/J	10	13.9	20.2	0.5	857	11	44.6	1.2	48.5	2.1	198	5
SM/J	10	15.4	14.1	0.3	881	25	62.6	1.6	47.1	2.3	222	7
WSB/EiJ	10	14.9	14.3	0.3	744	28	53.8	1.9	40.8	1.7	201	4

Definition of abbreviations: BW, body weight; sC_L, specific static compliance of the lung [C_L/TLC in ml (μ l/cm H₂O/ml TLC)]; SE, standard error; TLC, total lung capacity; TLC/BW, specific total lung capacity; V_D, dead space volume. *Values are means.

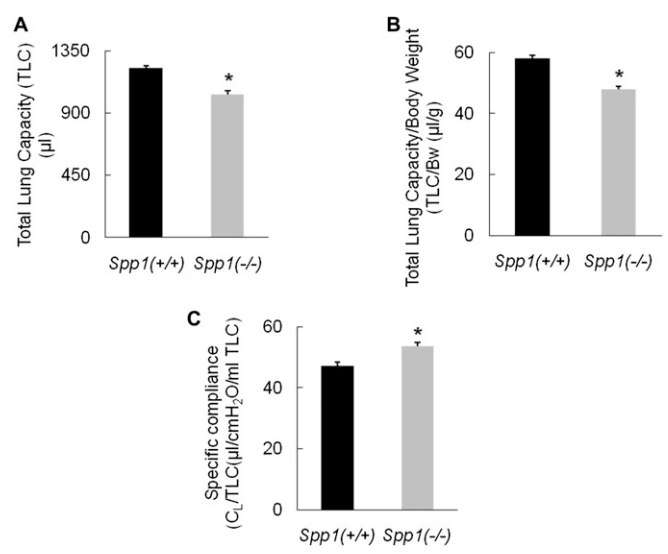


Figure 3. Lung function measurements of secreted phosphoprotein 1–deficient [$Spp1^{(-/-)}$] mice compared with strain-matched control [$Spp1^{(+/+)}$] mice. (A) $Spp1^{(-/-)}$ mice have 15% decreased total lung capacity (TLC) [$Spp1^{(-/-)} = 1,034 \pm 25$ versus $Spp1^{(+/+)} = 1,220 \pm 22$ μ]. (B) $Spp1^{(-/-)}$ mice have 17% decreased specific TLC (TLC/body weight) ($Spp1^{(-/-)} = 48 \pm 1$ versus $Spp1^{(+/+)} = 58 \pm 1$ μ/g). (C) $Spp1^{(-/-)}$ mice have 14% increased specific compliance (sC_L) compared with $Spp1^{(+/+)}$ mice ($Spp1^{(-/-)} = 54 \pm 1$ versus $Spp1^{(+/+)} = 47 \pm 1$ μ/cm H₂O/ml). Values are mean ± SE (n = 8 mice/strain; age = 12–14 wk). Statistical significance (*P < 0.001) was determined by ANOVA and by all pairwise comparisons procedure (Holm-Sidak method).

Transcriptomic analysis

To assess the lung transcriptomic profile during P14 (peak alveologenesis phase) and P28 (completion of alveologenesis and lung development), microarray analysis was performed with mRNA isolated from

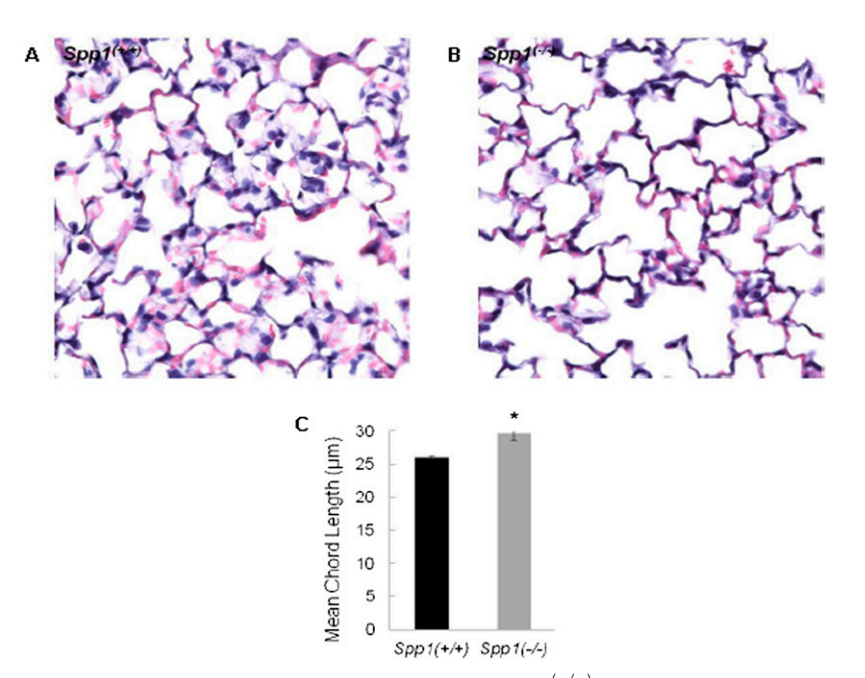


Figure 4. Comparison of alveolar air space size between $Spp1^{(-/-)}$ and strain-matched control $[Spp1^{(+/+)}]$ mice at the age of 4 weeks when alveolarization is completed. (A) $Spp1^{(+/+)}$; (B) $Spp1^{(-/-)}$. Lung morphometric analysis revealed 14% increased mean chord length in $Spp1^{(-/-)}$ mice (L_m: $29.7 \pm 0.3 \, \mu$ m) compared with $Spp1^{(+/+)}$ mice (L_m: $26.0 \pm 0.3 \, \mu$ m) (C). Values are mean $\pm SE$ ($n = 5 \, mice/strain$). Statistical significance (*P < 0.05) was determined by ANOVA and by all pairwise comparisons procedure (Holm-Sidak method).

 $Spp1^{(-/-)}$ and $Spp1^{(+/+)}$ mouse lung. P14 and P28 were chosen based on reduced SPP1 transcript expression pattern in JF1/ Msf lungs compared with C3H/HeJ. Initially, we examined the transcripts that were increased or decreased at P14 or P28 (n = 7,384). These transcripts were significantly enriched in genes associated with gene onotogy category GO:0030324 lung development (n = 132 significant of 387 in the category; P = 1.0E-08) (Figure 5). These 132 transcripts grouped into four clusters including transcripts that decreased at P14 and P28, increased at P14 and decreased at P28, decreased at P14 and increased at P28, or increased at P14 and P28. These clusters were analyzed for enrichment in transcripts associated with canonical pathways using Ingenuity Pathway Analysis. The top pathway for each cluster included retinoic acid receptor activation (P = 1.7E-06), aryl hydrocarbon receptor signaling (P = 1.4E-04), notch signaling (P = 7.8E-04), bone morphogenetic protein signaling pathway (P = 1.8E-0.8), and fibroblast growth factor (FGF) signaling (P = 1.5E-0.6), respectively.

Transcripts \geq 1.5-fold increased or \leq 1.5-fold decreased in $Spp1^{(-'-')}$ lung as compared with $Spp1^{(+'+')}$ were analyzed for enriched pathways using Database for Annotation, Visualization, and Integrated Discovery (DAVID) (39, 40). The enriched categories of Gene Ontogeny (GO) molecular function, GO biological process, GO cell component, and Kyoto Encyclopedia of Genes and Genomes (KEGG) pathways were determined. Ten transcripts with the greatest difference between strains at age P14 or P28 in each of these GO/KEGG categories are listed in Tables 2–5.

The GO/KEGG categories at P14 containing increased transcripts (n = 738 transcripts with unique Entrez Gene ID) in $Spp1^{(-/-)}$ mouse lung were protein tyrosine kinase activity, blood vessel morphogenesis, and cell projection (Table 2). Several genes or gene products in these pathways have been associated with abnormal lung development or lung disease (e.g., asthma, or COPD). Noteworthy transcripts in these categories/pathways included FGF receptor 3 (FGFR3) (41); hypoxia inducible factor 1, α subunit (HIF1A) (42); intelectin 1 (ITLN1) (43, 44); and heme oxygenase 1 (HMOX1) (45, 46).

The GO/KEGG categories at P14 containing decreased transcripts (n = 388) in $Spp1^{(-/-)}$ mouse lung were peptidase

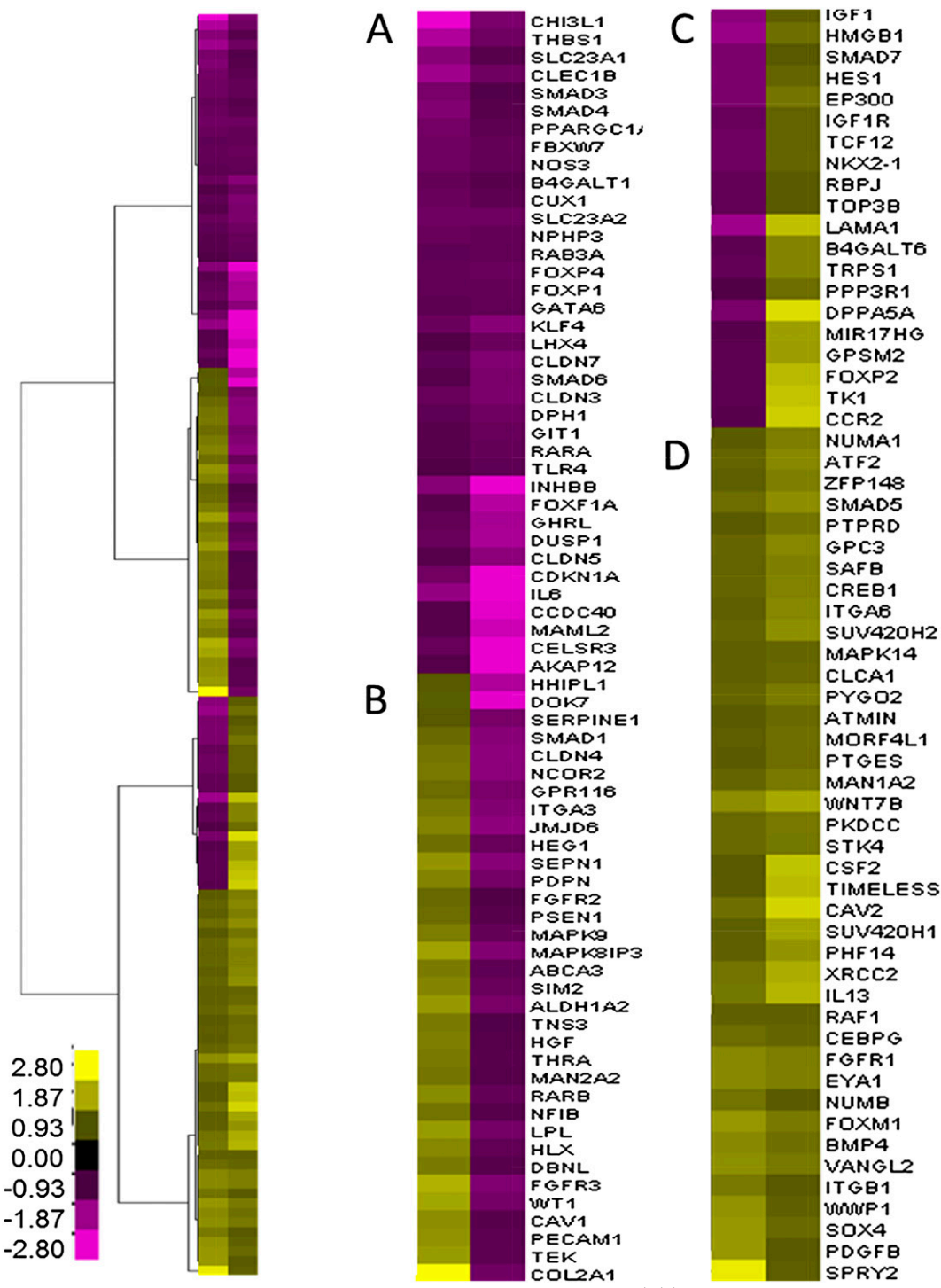


Figure 5. Hierarchical clustering of altered transcripts associated with lung development in $Spp1^{(-/-)}$ compared with strain-matched control $[Spp1^{(+/+)}]$ mice at P14 or P28. Transcripts were significantly enriched in genes associated with lung development (n = 132 significant of 387 in the category;) P = 1E-08). Four major clusters were identified: decreased at P14 and P28 (A), increased at P14 and decreased at P28 (B), decreased at P14 and increased at P28 (B), or increased at P14 and P28 (D). Significant difference in transcript levels for the microarray data was analyzed using ANOVA (P < 0.05). Fold change color scale is adjacent to the heat map. Values are means (n = 6-14 mice/strain), with yellow denoting increased and purple denoting decreased in $Spp1^{(-/-)}$ compared with strain-matched control $(Spp1^{(+/+)})$ mice. Each row represents a gene, and each column represents mean difference for P14 or P28.

Table 2. Increased Lung Transcripts in Secreted Phosphoprotein 1-Deficient Mice at Postnatal Day 14

Gene Symbol	Entrez Gene ID	Fold Change	P Value	Description	Enrichment Score		
Molecular function: GO:0004713 protein tyrosine kinase activity							
Dyrk1a	13548	2.24	0.002	dual-specificity tyrosine-(Y)-phosphorylation regulated kinase 1a			
Ltk	17005	2.11	0.028	leukocyte tyrosine kinase			
Fgfr3	14184	1.95	< 0.001	fibroblast growth factor receptor 3			
Map2k6	26399	1.82	0.005	mitogen-activated protein kinase kinase 6			
Cdc7	12545	1.74	0.034	cell division cycle 7 (Saccharomyces cerevisiae)			
Tyk2	54721	1.64	< 0.001	tyrosine kinase 2			
Bĺk	12143	1.59	0.029	B lymphoid kinase			
Epha5	13839	1.59	< 0.001	Eph receptor A5			
Ntrk2	18212	1.55	0.002	neurotrophic tyrosine kinase, receptor, type 2			
Ephb3	13845	1.51	< 0.001	Eph receptor B3			
	s: GO:0048514 blo				2.3		
Hif1a	15251	2.14	0.005	hypoxia inducible factor 1, alpha subunit	2.0		
Tbx20	57246	2.09	0.001	T-box 20			
Wt1	22431	1.83	0.029	Wilms tumor 1 homolog			
Hmox1	15368	1.69	0.001	heme oxygenase (decycling) 1			
Foxm1	14235	1.67	0.027	forkhead box M1			
Cav1	12389	1.58	0.018	caveolin 1, caveolae protein			
Ovol2	107586	1.57	< 0.001	ovo-like 2 (Drosophila)			
Ntrk2	18212	1.55	0.002	neurotrophic tyrosine kinase, receptor, type 2			
DII4	54485	1.55	0.002	delta-like 4 (Drosophila)			
Ccbe1	320924	1.51	0.014	collagen and calcium binding EGF domains 1			
Tnni3	21954	1.50	0.014	troponin I, cardiac 3			
			0.043	troportin i, cardiac 3	.8		
	ent: GO:0042995 c		0.010	intelectin 1 (galactofurances binding)	.0		
Itln1	16429 19132	4.32 2.12	0.018 0.027	intelectin 1 (galactofuranose binding)			
Prph	320051	2.12	0.027	peripherin exophilin 5			
Exph5	17898		0.005				
Myl7		1.86		myosin, light polypeptide 7, regulatory			
Dynlt1c	1E+08	1.80	< 0.001	dynein light chain Tctex-type 1C			
Ctnnd1	12388	1.79	0.020	catenin (cadherin associated protein), delta 1			
Dpysl5	65254	1.71	0.001	dihydropyrimidinase-like 5			
C2cd3	277939	1.67	0.050	C2 calcium-dependent domain containing 3			
Cyth3	19159	1.67	0.006	cytohesin 3			
Tesc	57816		0.024	tescalcin			
KEGG pathway: i	mmu05414: dilated				1.9		
Grik2	14806	2.68	0.001	glutamate receptor, ionotropic, kainate 2 (beta 2)			
Myh6	17888	2.22	0.017	myosin, heavy polypeptide 6, cardiac muscle, alpha			
Mybpc3	17868	2.09	0.004	myosin binding protein C, cardiac			
Atp1a2	98660	1.88	0.006	ATPase, Na+/K+ transporting, alpha 2 polypeptide			
Adrb1	11554	1.83	< 0.001	adrenergic receptor, beta 1			
Tnnc1	21924	1.80	0.035	troponin C, cardiac/slow skeletal			
Adrb3	11556	1.72	< 0.001	adrenergic receptor, beta 3			
Actg1	11465	1.70	0.003	actin, gamma, cytoplasmic 1			
Atp2a2	11938	1.66	0.004	ATPase, Ca ²⁺ transporting, cardiac muscle, slow twitch 2			
Tnni3	21954	1.50	0.045	troponin I, cardiac 3			

Definition of abbreviations: GO, gene ontogeny; KEGG, Kyoto Encyclopedia of Genes and Genomes.

activity, response to wounding, extracellular space, and cytokine-cytokine receptor interaction (Table 3). Noteworthy transcripts in these categories/pathways included matrix metalloproteinase 25 (MMP25; aka MT-MMP6) (47), thrombospondin 1 (THBS1) (48, 49), Toll-like receptor 1 (TLR1) (50, 51), TLR5 (52), chitinase 3-like 1 (CHIL3L1) (53, 54), and IL 12b (IL12B) (55, 56).

The GO/KEGG categories at P28 containing increased transcripts (n = 1,436) in $Spp1^{(-/-)}$ mouse lung were zinc ion

binding, regulation of transcription, microtubule cytoskeleton, and cell cycle (Table 4). Noteworthy transcripts in these categories/pathways included forkhead box P2 (FOXP2) (57), midline 1 (MID1) (58), metal response element binding transcription factor 1 (MTF1) (59), SRY-box containing gene 9 (SOX9) (60), SOX5 (61), nuclear factor I/A (NFIA) (62), and spermassociated antigen 17 (SPAG17) (63).

The GO/KEGG categories at P28 containing decreased transcripts (n = 1,161)

in *Spp1*^(-/-) mouse lung were protein kinase activity, protein kinase cascade, cell-cell junction, and tight junction (Table 5). Noteworthy transcripts in these categories/pathways included casein kinase 1, epsilon (CSNK1E) (64), mitogenactivated protein kinase 6 (MAPK6; a.k.a. ERK3) (65), mechanistic target of rapamycin (serine/threonine kinase) (MTOR) (66), oncostatin M (OSM) (67, 68), TLR6 (69), mucin 20 (MUC20) (70, 71), MAD homolog 1 (SMAD1) (72, 73),

Table 3. Decreased Lung Transcripts in Secreted Phosphoprotein 1-Deficient Mice at Postnatal Day 14

Gene Symbol	Entrez Gene ID	Fold Change	P Value	Description	Enrichment Score
Molecular function	on GO:0008233 pe	otidase activity			2.4
Adamts4	240913	-5.8	0.005	a disintegrin-like and metallopeptidase (reprolysin type) with thrombospondin type 1 motif, 4	
Adam28	13522	-2.5	0.007	a disintegrin and metallopeptidase domain 28	
Agbl3	76223	-2.5	0.001	ATP/GTP binding protein-like 3	
Mmel1	27390	-2.3	0.026	membrane metallo-endopeptidase-like 1	
Adamdec1	58860	-2.2	0.044	ADAM-like, decysin 1	
Qpct	70536	-1.8	0.042	glutaminyl-peptide cyclotransferase (glutaminyl cyclase)	
Acr	11434	-1.7	0.037	acrosin prepropeptide	
Ecel1	13599	-1.7	0.025	endothelin converting enzyme-like 1	
Mmp25	240047	-1.6	0.004	matrix metallopeptidase 25	
Usp36	72344	-1.5	0.003	ubiquitin specific peptidase 36	
	s GO:0009611 res				1.5
Gp9	54368	-2.4	0.012	glycoprotein 9 (platelet)	
Thbs1	21825	-2.1	0.010	thrombospondin 1	
Tnfrsf1b	21938	-2.1	< 0.001	tumor necrosis factor receptor superfamily, member 1b	
Tlr1	21897	-2.0	0.033	Toll-like receptor 1	
P2ry12	70839	-1.9	0.003	purinergic receptor P2Y, G-protein coupled 12	
Pf4	56744	-1.7	< 0.001	platelet factor 4	
Tlr5	53791	-1.6	0.048	Toll-like receptor 5	
Hps5	246694	-1.6	0.032	Hermansky-Pudlak syndrome 5 homolog (human)	
Treml1	71326	-1.6	0.017	triggering receptor expressed on myeloid cells-like 1	
Ccl19	24047	-1.5	0.029	chemokine (C-C motif) ligand 19	2.2
	ent GO:0005615 ex				2.8
Afm	280662	-4.6	0.001	afamin	
Enpp1	18605	-2.9	0.045	ectonucleotide pyrophosphatase/ phosphodiesterase 1	
Chi3l1	12654	-2.8	0.024	chitinase 3-like 1	
Cilp	214425	-2.8	0.005	cartilage intermediate layer protein, nucleotide pyrophosphohydrolase	
Spon2	100689	-2.7	0.016	spondin 2, extracellular matrix protein	
Apoc2	11813	-2.7	0.025	apolipoprotein C-II	
Adam28	13522	-2.5	0.007	a disintegrin and metallopeptidase domain 28	
Gdf3	14562	-2.5	0.029	growth differentiation factor 3	
Mmp8	17394	-2.4	0.034	matrix metallopeptidase 8	
Grp	225642	-2.3	0.004	gastrin releasing peptide	
	nmu04060: cytokir				1.8
Ccr8	12776	-2.8	0.014	chemokine (C-C motif) receptor 8	
Ccl7	20306	-2.4	0.047	chemokine (C-C motif) ligand 7	
Cxcr2	12765	-2.3	0.010	chemokine (C-X-C motif) receptor 2	
Tnfrsf13c	72049	-2.3	0.038	tumor necrosis factor receptor superfamily, member 13c	
Tnfrsf9	21942	-2.1	0.039	tumor necrosis factor receptor superfamily, member 9	
Ccl12	20293	-2.1	0.041	chemokine (C-C motif) ligand 12	
II12b	16160	-2.0	< 0.001	interleukin 12b	
Mpl	17480	-1.7	0.012	myeloproliferative leukemia virus oncogene	
Pf4	56744	-1.7	>0.001	platelet factor 4	
Inhbb	16324	-1.6	0.004	inhibin beta-B	

FGFR3, protein phosphatase 2 (formerly 2A), catalytic subunit, α isoform (PPP2CA) (74, 75), claudin 3 (CLDN3), CLDN4, CLDN5, CLDN7 (76–78), and lethal giant larvae homolog 2 (Drosphila) (LLGL2) (79, 80).

To further assess transcripts associated with lung development, transcripts encoding IGF1, WNT5A, HHIP, notch 1 (NOTCH1), and CD44 antigen (CD44) were assessed by qRT-PCR. As compared with P14 *Spp1*^(+/+) mice, lung IGF1, WNT5A, HHIP, and

NOTCH1 transcripts decreased in P14 $Spp1^{(-/-)}$ mice (Figure 6A). At P28, only HHIP was decreased in $Spp1^{(-/-)}$ compared with $Spp1^{(+/+)}$ mouse lung (Figure 6A).

Discussion

Rapid identification of functional candidate genes in mice has been valuable in providing insights into human lung development. In this study, we assessed the functionality of *Spp1* located within another QTL for lung function for its plausible role as a pulmonary function determinant in mice.

Mammalian lung development is a precisely orchestrated process that involves lung airway branching morphogenesis and alveolarization along with angiogenesis and vasculogenesis during embryonic and postnatal periods (81). Severe impairments during any

Table 4. Increased Lung Transcripts in Secreted Phosphoprotein 1 Deficient Mice at Postnatal Day 28

Gene Symbol	Entrez Gene ID	Fold Change	P Value	Description	Enrichment Score:		
Molecular function: GO:0008270 zinc ion binding							
Rag1	19373	11.07	0.013	recombination activating gene 1			
Zfp14	243906	4.13	0.001	zinc finger protein 14			
Trim59	66949	3.38	< 0.001	tripartite motif-containing 59			
Birc5	11799	2.82	0.016	baculoviral IAP repeat-containing 5			
Snai2	20583	2.46	0.033	snail homolog 2 (Drosophila)			
Foxp2	114142	2.06	0.024	forkhead box P2			
Mid1	17318	1.97	0.034	midline 1			
Naip6	17952	1.94	0.013	NLR family, apoptosis inhibitory protein 6			
Rfwd2	26374	1.77	0.004	ring finger and WD repeat domain 2			
Mtf1	17764	1.72	< 0.001	metal response element binding transcription			
				factor 1			
Biological proces	ss: GO:0045449 reg	gulation of trans	cription		14.3		
Dnmt3a	13435	2.80	0.010	DNA methyltransferase 3A			
Runx1	12394	2.67	0.008	runt related transcription factor 1			
Sox9	20682	2.52	0.005	SRY-box containing gene 9			
Ccna2	12428	2.39	0.044	cyclin A2			
Sox5	20678	2.16	0.011	SRY-box containing gene 5			
Myb	17863	2.15	0.009	myeloblastosis oncogene			
Egr3	13655	2.02	0.042	early growth response 3			
Maf	17132	1.98	0.028	avian musculoaponeurotic fibrosarcoma (v-maf)			
				AS42 oncogene homolog			
Nfia	18027	1.80	0.011	nuclear factor I/A			
E2f2	242705	1.74	0.017	E2F transcription factor 2			
	ent: GO:0015630 n				7.7		
Tube1	71924	3.63	0.001	epsilon-tubulin 1			
Aurka	20878	3.46	< 0.001	aurora kinase A			
Kifc1	1E+08	2.66	0.012	kinesin family member C1			
Spag17	74362	2.36	0.005	sperm associated antigen 17			
Tubd1	56427	2.22	0.001	tubulin, delta 1			
Cep55	74107	2.01	< 0.001	centrosomal protein 55			
Haus8	76478	1.95	0.006	4HAUS augmin-like complex, subunit 8			
Rpgrip1I	244585	1.83	0.021	Rpgrip1-like			
Ttll7	70892	1.78	0.041	tubulin tyrosine ligase-like family, member 7			
C2cd3	277939	1.72	0.016	C2 calcium-dependent domain containing 3			
	mmu04110 cell cy		0.010	52 53.3idili dopondoni domani oontaning o	2.9		
Cdk1	12534	2.92	0.036	cyclin-dependent kinase 1	2.0		
Bub1	12235	2.89	0.000	budding uninhibited by benzimidazoles 1 homolog			
Dubi	12200	2.00	0.001	(Saccharomyces cerevisiae)			
Skp2	27401	2.70	0.002	S-phase kinase-associated protein 2 (p45)			
Ccnb1	268697	2.47	0.002	cyclin B1			
Ccna2	12428	2.39	0.004	cyclin A2			
Chek2	50883	2.25	0.044	CHK2 checkpoint homolog (Schizosaccharomyces			
OHERZ	30003	۷.۷	0.043	pombe)			
Cdc20	107995	2.25	0.006	cell division cycle 20 homolog (S. cerevisiae)			
Plk1	18817	2.25	0.008	polo-like kinase 1 (Drosophila)			
Cdc25c	12532	2.10	0.008	cell division cycle 25 homolog C (S. pombe)			
Anapc10	68999	2.09 1.81	0.036	anaphase promoting complex subunit 10			
ліарсто	00999	1.01	0.011	anaphase promoting complex subunit 10			

developmental stage can result in bronchopulmonary dysplasia, neonatal respiratory failure, and death (82). However, mild structural or functional defects due to aberrant lung development (83) may increase susceptibility to respiratory diseases (COPD, cystic fibrosis, or asthma) that may be clinically detectable only during childhood or later in life through pulmonary function testing (84–87). Therefore, it is important to detect genetic abnormalities that can affect early

fetal and postnatal lung development; postnatal lung growth and maturation; and lung injury, repair, and remodeling processes (84–90).

In mice, alveolarization takes place between P5 and P30 and is controlled by finely integrated and mutually regulated networks of transcriptional factors, growth factors, matrix components, and physical forces (9, 89–92). Factors that adversely affect the developing lung include premature birth, oxygen exposure, early corticosteroidal exposure, dysregulated growth factor (IGF, WNT, NOTCH, BMP/ TGFB, FGF, PDGF, VEGFA) signaling, and abnormal regulation or injury of the pulmonary capillary vasculature. Individually and cumulatively, these factors can result in hypoplasia of the alveolar epithelial surface, with a resulting deficiency in pulmonary function (e.g., decreased TLC or increased C_L).

As compared with C3H/HeJ mice, lung SPP1 transcript decreased in JF1/Msf mice,

Table 5. Decreased Lung Transcripts in Secreted Phosphoprotein 1-Deficient Mice at Postnatal Day 28

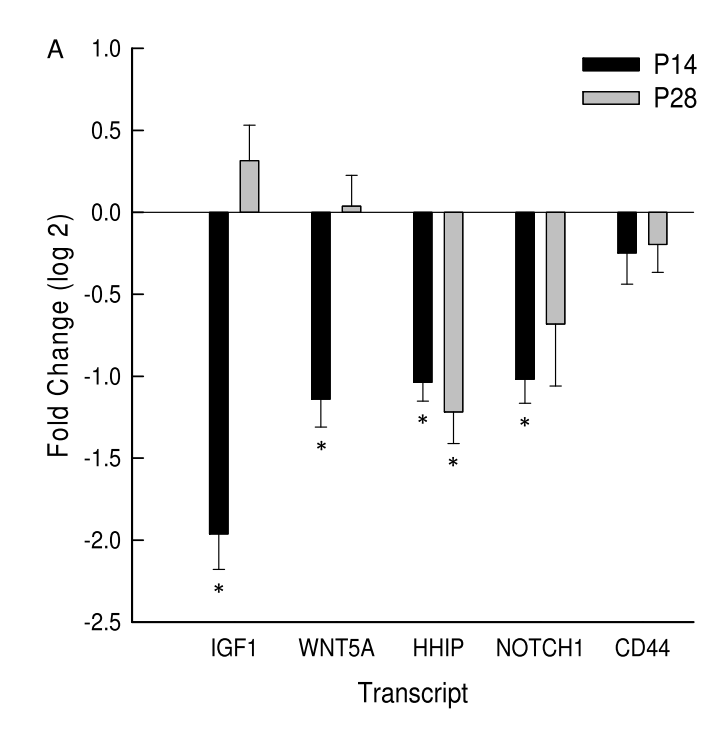
Gene Symbol	Entrez Gene ID	Fold Change	P Value	Description	Enrichment Score
Molecular function	on: GO:0004672 pr	otein kinase acti		2.4	
Taok2	381921	-3.12	0.001	TAO kinase 2	
Phkg1	18682	-3.03	0.003	phosphorylase kinase gamma 1	
Tnk1	83813	-2.70	0.015	tyrosine kinase, non-receptor, 1	
Csnk1e	27373	-2.64	0.002	casein kinase 1, epsilon	
Mapk6	50772	-2.49	0.006	mitogen-activated protein kinase 6	
Plk3	12795	-2.19	< 0.001	polo-like kinase 3 (Drosophila)	
Sgk2	27219	-2.16	0.025	serum/glucocorticoid regulated kinase 2	
Irak2	108960	-2.15	0.025	interleukin-1 receptor-associated kinase 2	
Mtor	56717	-2.14	0.005	mechanistic target of rapamycin (serine/threonine kinase)	
Trib1	211770	-2.10	< 0.001	tribbles homolog 1 (Drosophila)	
	s: GO:0007243 pro			S (-17 -77	2.4
Gna13	14674	-3.06	< 0.001	guanine nucleotide binding protein, alpha 13	
Osm	18413	-2.82	0.005	oncostatin M	
Tlr6	21899	-2.62	0.007	Toll-like receptor 6	
Muc20	224116	-2.18	0.048	mucin 20	
Irak2	108960	-2.15	0.025	interleukin-1 receptor-associated kinase 2	
Ghrl	58991	-2.00	0.005	ghrelin	
Edn1	13614	-1.99	0.012	endothelin 1	
Pxn	19303	-1.71	0.005	paxillin	
Smad1	17125	-1.65	0.045	MAD homolog 1 (Drosophila)	
Dapk3	13144	-1.62	0.045	death-associated protein kinase 3	
Fgfr3	14184	-1.53	0.033	fibroblast growth factor receptor 3	
	ent: GO:0005911 c		0.000	nordolast grown ractor receptor e	2.5
Myl2	17906	-8.71	0.027	myosin, light polypeptide 2, regulatory, cardiac, slow	
Nrap	18175	-3.29	0.003	nebulin-related anchoring protein	
Myh7	140781	-2.96	0.002	myosin, heavy polypeptide 7, cardiac muscle, beta	
Ppp2ca	19052	-2.60	<0.001	protein phosphatase 2 (formerly 2A), catalytic subunit, alpha isoform	
Csnk2a2	13000	-2.40	0.003	casein kinase 2, alpha prime polypeptide	
Shroom3	27428	-2.27	0.016	shroom family member 3	
Pcp4	18546	-2.10	0.006	Purkinje cell protein 4	
Prkcz	18762	-2.07	0.005	protein kinase C, zeta	
Ppp2r2b	72930	-2.05	0.039	protein phosphatase 2 (formerly 2A), regulatory subunit B (PR 52), beta isoform	
Cldn23	71908	-1.88	0.023	claudin 23	
KEGG pathway:	mmu04530: tight ju	unction			1.9
Exoc4	20336	-1.86	0.032	exocyst complex component 4	
Gja4	14612	-1.81	0.001	gap junction protein, alpha 4	
Pard6b	58220	-1.77	0.002	par-6 (partitioning defective 6) homolog beta (Caenorhabditis elegans)	
Myh9	17886	-1.77	0.002	myosin, heavy polypeptide 9, nonmuscle	
Cldn4	12740	-1.70	0.039	claudin 4	
Ahnak	66395	-1.70	0.020	AHNAK nucleoprotein (desmoyokin)	
Cldn5	12741	-1.69	0.006	claudin 5	
Llgl2	217325	-1.58	0.017	lethal giant larvae homolog 2 (Drosophila)	
Cldn7	53624	-1.55	0.016	claudin 7	
Cldn3	12739	-1.51	0.004	claudin 3	

a strain with decreased lung function. This decrease was noted from P14 onward, which is the peak phase of alveologenesis in mice. Alveolization takes place by the process of septation of primitive saccules into smaller units during late gestation in humans and postnatally in mice. During this period secondary crests develop and extend to form alveoli, resulting in increased surface area for gaseous exchange. Alveolization defects result in large alveoli, reminiscent of the

abnormality found in emphysema but with less overt destruction. Indicative of impaired alveologeneis, $Spp1^{(-/-)}$ mice had increased alveolar size (i.e., $L_{\rm m}$) that was detectable as early as 4 weeks of age when the process is just completed. Increased alveolar size also implicates reduced alveolar surface area (S = $4V/L_{\rm m}$) for gas exchange (93). At around 4 weeks of age, the lung development is complete, and the lung assumes the structure of an adolescent lung. Thus, P28 is

an important screening stage for evaluating postnatal lung development (21).

Several genetic variants in the *Spp1* proximal promoter differ between C3H/HeJ and JF1/Msf mice. Previously, Sowa and colleagues (34) identified a 13-bp insertion (rs234069704) at position -130 located at the 3' end of the RUNX2 binding site. This insertion increased transcriptional responsiveness to RUNX2 in the C3H/HeJ promoter as compared with that of the



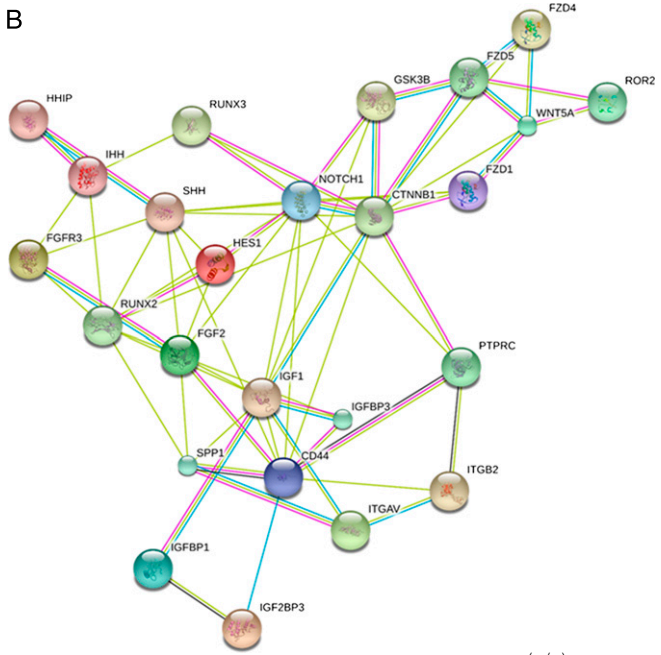


Figure 6. Transcripts associated with lung development are altered in $Spp1^{(-/-)}$ as compared with strain-matched control [$Spp1^{(+/+)}$] mice at P14 or P28. (A) Lung mRNA was isolated, and transcript levels were determined by quantitative RT-PCR (qRT-PCR). Values are mean \pm SE (n=6–14 mice/strain). Statistical significance (*P<0.05) was determined by ANOVA and by all pairwise comparisons procedure (Holm-Sidak method). (B) Protein–protein interaction network of SPP1 with proteins associated with lung development. CTNNB1, catenin (cadherin associated protein), β 1; CD44, CD44 antigen; FGF2, fibroblast growth factor 2; FGFR3, fibroblast growth factor receptor 3; FZD1, frizzled class receptor 1; FZD4, frizzled class receptor 4; FZD5, frizzled class receptor 5; GSK3B, glycogen synthase kinase 3 β; HES1, hes family bHLH transcription factor 1; HHIP, hedgehog interacting protein; IGF1, insulin-like growth factor 1; IGFBP1, insulin-like growth factor binding protein 3; IGF2BP3, insulin-like growth factor binding protein 3; IHH, Indian hedgehog; ITGAV, integrin α V; ITGB2, integrin β 2; NOTCH1, notch 1; PTPRC, protein tyrosine phosphatase, receptor type, C (aka CD45); ROR2, receptor tyrosine kinase-like orphan receptor 2; RUNX2, runt-related transcription factor 2; RUNX3,runt-related transcription factor 3; SHH, sonic hedgehog; WNT5A, wingless-related MMTV integration site 5A.

C57BL/6J promoter. Because JF1/Msf mice, similar to C57BL/6J mice, lack the poly-T insertions, the C3H/HeJ *Spp1* promoter would also be more responsive to RUNX2 than the JF1/Msf promoter. In addition, we examined whether SNPs at position -158 (rs264140167) or -198 (rs47003578) could alter putative binding sites. The C3H/HeJ T rs264140167 allele at -158 in the *Spp1* promoter enhanced nuclear protein–target DNA binding capacity. The C3H/HeJ T allele forms an additional putative RUNX2 binding site not present in the JF1/Msf G allele.

Several variants in the human SPP1 promoter have been identified and are functional. For example, variants at -66(rs28357094), -156 (rs11439060), and -443 (rs11730582) bp from the transcriptional start site can modify activation by Sp1 transcription factor (SP1), RUNX2, and v-myb avian myeloblastosis viral oncogene homolog, respectively (94, 95). The -156 bp rs11439060 variant is an insertion (-/G) that provides a functional RUNX2 binding site and is near the -158SNP in the mouse genome, which also provides a putative RUNX2 binding site in C3H/HeJ mice (Figure E5). Human promoter SNPs also have been reported as autoimmune risk variants for systemic lupus erythematosus (96, 97), systemic sclerosis (98), inflammatory bowel disease (99), and rheumatoid arthritis (100). RUNX2-mediated SPP1 promoter activity can be inhibited by histone deacetylase 1 (101), and RUNX transcription factors have been associated with increased risk of asthma in children with in utero smoke exposure (102, 103).

Similar to what we have reported previously with primary human normal lung fibroblast and with the A549 lung epithelial cell line (27), SPP1 induced mouse MLE-15 cell proliferation. SPP1 also alters fibroblast migration (27), further supporting its likely role in lung development. The smaller TLC and higher C_L in $Spp1^{(-/-)}$ mice could be a result of impaired alveologenesis. Inasmuch as SPP1 can influence the proliferation of type II-like epithelial cells and lung fibroblasts, the altered lung function in $Spp1^{(-/-)}$ mice may be due to increased alveoloar size or diminished tissue elastic recoil of the lungs. Therefore, impaired alveologenesis could explain the decreased TLC and increased C_L observed in SPP1-deficient mice.

Lung microarray analysis revealed numerous differences in transcripts critical to lung development in $Spp1^{(-/-1)}$ mice as compared with strain-matched control mice. GO categories of molecular function, biological process, and cell component and KEGG pathways contained transcripts associated with lung development (P14 increased FGFR3, HIF1A; P14 decreased THBS1; P28 increased FOXP2, MTF1, SOX5, SOX9, NFIA, and SPAG17; P28 decreased CSNK1E, MAPK6, SMAD1, FGFR3, PPP2CA, CLDN3, CLDN4, CLDN5, CLDN7, and LLGL2) or lung diseases including asthma (P14 increased ITLN1; P14 decreased CHIL3L1 and IL12B; P28 increased MID1; P28 decreased MTOR, TLR6 and PPP2CA) and COPD (P14 increased HMOX1; P14 decreased MMP25; P28 increased SOX5). These altered transcripts suggest that SPP1 interacts with a wide range of proteins that regulate normal development and supports the hypothesis that abnormal development is a risk factor for chronic respiratory diseases.

Lung IGF1, HHIP, WNT5A, and NOTCH1 transcripts decreased in P14 $Spp1^{(-/-)}$ mice as determined by qRT-PCR analysis. These transcripts encoded proteins that formed an interactive network that included interactions of SPP1 with IGF1, RUNX2, CD44, FGF2, and integrin α V

(Figure 6B). Other proteins were required to include HHIP, WNT5A, and NOTCH1 in the interactome that includes SPP1, suggesting that SPP1 is associated with these transcripts through indirect interactions. In addition, the validated transcripts encode proteins that have key roles in the other regulatory networks that control lung development. In mice, IGF1 regulates airspace formation by promoting an elastogenic lineage in undifferentiated mesenchymal cells (104) and is critical for lung development (105).

HHIP regulates the hedgehog pathway implicated in development and repair in multiple tissues (106). Gene-targeted HHIP-deficient mice display defective airway branching morphogenesis and lung hypoplasia that results in death due to respiratory failure at birth (107). In humans, SNPs located near *HHIP* have been associated with lung development and growth (108) and COPD (10–16, 107–111).

In mice, disruption of *Wnt5a* results in distinct truncation of the trachea and overexpansion of the distal respiratory airways (112), whereas overexpression of WNT5A interferes with epithelial–mesenchymal crosstalk, resulting in reduced airway branching and dilated distal airways (113). In addition, hedgehog and FGF signaling were altered

in WNT5A overexpressing mice (113), clearly indicating its role in lung development.

NOTCH signaling is critical for normal balance of differentiated cell fates in the airway epithelium (114, 115). Transgenic mice expressing a constitutively activated NOTCH1 in the lung epithelium have fewer ciliated cells and more mucin-producing cells, suggesting its role in the lineage determination of secretory or nonsecretory cells (116, 117). The NOTCH1 pathway has been implicated in SPP1 transcription in HES1-transfected cells and can be inhibited by AML-1/ETO, an inhibitor of RUNX2 (33).

To summarize, mice with decreased SPP1 have smaller but more compliant lungs, which is likely due to impaired alveologenesis. This is accompanied by altered expression patterns of key lung developmental transcripts in P14 Spp1^(−/−) mice (during peak alveologenesis phase) and increased alveolar airspace detectable in P28 Spp1^(−/−) mice (when alveologenesis is nearly complete). Together, these findings support a key role for SPP1 in lung development, which adds to its known role in chronic lung disease. ■

Author disclosures are available with the text of this article at www.atsjournals.org.

References

- Mathers CD, Loncar D. Projections of global mortality and burden of disease from 2002 to 2030. PLoS Med 2006;3:e442.
- Burrows B, Knudson RJ, Lebowitz MD. The relationship of childhood respiratory illness to adult obstructive airway disease. Am Rev Respir Dis 1977;115:751–760.
- 3. Strachan D. Ventilatory function, height, and mortality among lifelong non-smokers. *J Epidemiol Community Health* 1992;46:66–70.
- Engstrom G, Hedblad B, Janzon L. Reduced lung function predicts increased fatality in future cardiac events: a population-based study. *J Intern Med* 2006;260:560–567.
- Bridevaux P, Gerbase M, Probst-Hensch N, Schindler C, Gaspoz J, Rochat T. Long-term decline in lung function, utilisation of care and quality of life in modified gold stage 1 COPD. *Thorax* 2008;63:768–774.
- Hirschhorn JN. Genomewide association studies: illuminating biologic pathways. N Engl J Med 2009;360:1699–1701.
- 7. Weiss ST. Lung function and airway diseases. Nat Genet 2010;42:14-16.
- 8. Beers MF, Morrisey EE. The three R's of lung health and disease: repair, remodeling, and regeneration. *J Clin Invest* 2011;121:2065–2073.
- Morrisey EE, Cardoso WV, Lane RH, Rabinovitch M, Abman SH, Ai X, Albertine KH, Bland RD, Chapman HA, Checkley W, et al. Molecular determinants of lung development. Ann Am Thorac Soc 2013;10: S12–S16.
- Wilk JB, Chen TH, Gottlieb DJ, Walter RE, Nagle MW, Brandler BJ, Myers RH, Borecki IB, Silverman EK, Weiss ST, et al. A genome-wide association study of pulmonary function measures in the framingham heart study. PLoS Genet 2009;5:e1000429.

- Repapi E, Sayers I, Wain LV, Burton PR, Johnson T, Obeidat M, Zhao JH, Ramasamy A, Zhai G, Vitart V, et al. Genome-wide association study identifies five loci associated with lung function. Nat Genet 2010;42:36–44.
- Hancock DB, Eijgelsheim M, Wilk JB, Gharib SA, Loehr LR, Marciante KD, Franceschini N, van Durme YM, Chen TH, Barr RG, et al. Meta-analyses of genome-wide association studies identify multiple loci associated with pulmonary function. Nat Genet 2010; 42:45–52.
- Imboden M, Bouzigon E, Curjuric I, Ramasamy A, Kumar A, Hancock DB, Wilk JB, Vonk JM, Thun GA, Siroux V, et al. Genome-wide association study of lung function decline in adults with and without asthma. J Allergy Clin Immunol 2012;129:1218–1228.
- Yao TC, Du G, Han L, Sun Y, Hu D, Yang JJ, Mathias R, Roth LA, Rafaels N, Thompson EE, et al. Genome-wide association study of lung function phenotypes in a founder population. J Allergy Clin Immunol 2013;133:248–255.
- Soler Artigas M, Loth DW, Wain LV, Gharib SA, Obeidat M, Tang W, Zhai G, Zhao JH, Smith AV, Huffman JE, et al. Genome-wide association and large-scale follow up identifies 16 new loci influencing lung function. Nat Genet 2011;43:1082–1090.
- Hancock DB, Artigas MS, Gharib SA, Henry A, Manichaikul A, Ramasamy A, Loth DW, Imboden M, Koch B, McArdle WL, et al. Genome-wide joint meta-analysis of snp and snp-by-smoking interaction identifies novel loci for pulmonary function. PLoS Genet 2012;8:e1003098.
- Eichler EE, Flint J, Gibson G, Kong A, Leal SM, Moore JH, Nadeau JH.
 Missing heritability and strategies for finding the underlying causes
 of complex disease. *Nat Rev Genet* 2010;11:446–450.

- Zuk O, Hechter E, Sunyaev SR, Lander ES. The mystery of missing heritability: genetic interactions create phantom heritability. *Proc Natl Acad Sci USA* 2012;109:1193–1198.
- Reinhard C, Eder G, Fuchs H, Ziesenis A, Heyder J, Schulz H. Inbred strain variation in lung function. *Mamm Genome* 2002;13: 429–437.
- Reinhard C, Meyer B, Fuchs H, Stoeger T, Eder G, Ruschendorf F, Heyder J, Nurnberg P, de Angelis MH, Schulz H. Genomewide linkage analysis identifies novel genetic loci for lung function in mice. Am J Respir Crit Care Med 2005;171:880–888.
- Ganguly K, Stoeger T, Wesselkamper SC, Reinhard C, Sartor MA, Medvedovic M, Tomlinson CR, Bolle I, Mason JM, Leikauf GD, et al. Candidate genes controlling pulmonary function in mice: transcript profiling and predicted protein structure. *Physiol Genomics* 2007;31: 410–421.
- Ganguly K, Depner M, Fattman C, Bein K, Oury TD, Wesselkamper SC, Borchers MT, Schreiber M, Gao F, von Mutius E, et al. Superoxide dismutase 3, extracellular (SOD3) variants and lung function. *Physiol Genomics* 2009;37:260–267.
- 23. Lindsey JY, Ganguly K, Brass DM, Li Z, Potts EN, Degan S, Chen H, Brockway B, Abraham SN, Berndt A, et al. c-Kit is essential for alveolar maintenance and protection from emphysema-like disease in mice. Am J Respir Crit Care Med 2011;183: 1644–1652.
- Dahl M, Bowler RP, Juul K, Crapo JD, Levy S, Nordestgaard BG. Superoxide dismutase 3 polymorphism associated with reduced lung function in two large populations. *Am J Respir Crit Care Med* 2008;178:906–912.
- Siedlinski M, van Diemen CC, Postma DS, Vonk JM, Boezen HM. Superoxide dismutases, lung function and bronchial responsiveness in a general population. *Eur Respir J* 2009;33: 986–992.
- 26. Sorheim IC, DeMeo DL, Washko G, Litonjua A, Sparrow D, Bowler R, Bakke P, Pillai SG, Coxson HO, Lomas DA, *et al.* Polymorphisms in the superoxide dismutase-3 gene are associated with emphysema in COPD. *COPD* 2010;7:262–268.
- Pardo A, Gibson K, Cisneros J, Richards TJ, Yang Y, Becerril C, Yousem S, Herrera I, Ruiz V, Selman M, et al. Up-regulation and profibrotic role of osteopontin in human idiopathic pulmonary fibrosis. PLoS Med 2005;2:e251.
- Schneider DJ, Lindsay JC, Zhou Y, Molina JG, Blackburn MR. Adenosine and osteopontin contribute to the development of chronic obstructive pulmonary disease. FASEB J 2010;24:70–80.
- Ashkar S, Weber GF, Panoutsakopoulou V, Sanchirico ME, Jansson M, Zawaideh S, Rittling SR, Denhardt DT, Glimcher MJ, Cantor H. Eta-1 (osteopontin): an early component of type-1 (cell-mediated) immunity. *Science* 2000;287:860–864.
- 30. Chabas D, Baranzini SE, Mitchell D, Bernard CC, Rittling SR, Denhardt DT, Sobel RA, Lock C, Karpuj M, Pedotti R, *et al.* The influence of the proinflammatory cytokine, osteopontin, on autoimmune demyelinating disease. *Science* 2001;294:1731–1735.
- 31. Liaw L, Birk DE, Ballas CB, Whitsitt JS, Davidson JM, Hogan BL. Altered wound healing in mice lacking a functional osteopontin gene (spp1). *J Clin Invest* 1998;101:1468–1478.
- 32. Trueblood NA, Xie Z, Communal C, Sam F, Ngoy S, Liaw L, Jenkins AW, Wang J, Sawyer DB, Bing OH, et al. Exaggerated left ventricular dilation and reduced collagen deposition after myocardial infarction in mice lacking osteopontin. Circ Res 2001;88:1080–1087.
- Shen Q, Christakos S. Vitamin D receptor, Runx2, and the Notch signaling pathway cooperate in the transcriptional regulation of osteopontin. J Biol Chem 2005;280:40589–40598.
- 34. Sowa AK, Kaiser FJ, Eckhold J, Kessler T, Aherrahrou R, Wrobel S, Kaczmarek PM, Doehring L, Schunkert H, Erdmann J, et al. Functional interaction of osteogenic transcription factors Runx2 and Vdr in transcriptional regulation of Opn during soft tissue calcification. Am J Pathol 2013;183:60–68.
- 35. Wikenheiser KA, Vorbroker DK, Rice WR, Clark JC, Bachurski CJ, Oie HK, Whitsett JA. Production of immortalized distal respiratory epithelial cell lines from surfactant protein c/simian virus 40 large tumor antigen transgenic mice. *Proc Natl Acad Sci USA* 1993;90: 11029–11033.

- Nguyen NM, Bai Y, Mochitate K, Senior RM. Laminin alpha-chain expression and basement membrane formation by MLE-15 respiratory epithelial cells. Am J Physiol Lung Cell Mol Physiol 2002; 282:L1004–L1011.
- Schulz H, Johner C, Eder G, Ziesenis A, Reitmeier P, Heyder J, Balling R. Respiratory mechanics in mice: strain and sex specific differences. *Acta Physiol Scand* 2002;174:367–375.
- Cartharius K, Frech K, Grote K, Klocke B, Haltmeier M, Klingenhoff A, Frisch M, Bayerlein M, Werner T. MatInspector and beyond: promoter analysis based on transcription factor binding sites. *Bioinformatics* 2005;21:2933–2942.
- Huang DW, Sherman BT, Lempicki RA. Systematic and integrative analysis of large gene lists using DAVID Bioinformatics Resources. Nat Protoc 2009;4:44–57.
- Huang DW, Sherman BT, Lempicki RA. Bioinformatics enrichment tools: paths toward the comprehensive functional analysis of large gene lists. *Nucleic Acids Res* 2009;37:1–13.
- Friedmacher F, Doi T, Gosemann JH, Fujiwara N, Kutasy B, Puri P. Upregulation of fibroblast growth factor receptor 2 and 3 in the late stages of fetal lung development in the nitrofen rat model. *Pediatr* Surg Int 2012;28:195–199.
- Shimoda LA, Semenza GL. HIF and the lung: role of hypoxia-inducible factors in pulmonary development and disease. Am J Respir Crit Care Med 2011:183:152–156.
- Pemberton AD, Rose-Zerilli MJ, Holloway JW, Gray RD, Holgate ST. A single-nucleotide polymorphism in intelectin 1 is associated with increased asthma risk. J Allergy Clin Immunol 2008;122:1033–1034.
- 44. Gu N, Kang G, Jin C, Xu Y, Zhang Z, Erle DJ, Zhen G. Intelectin is required for IL-13-induced monocyte chemotactic protein-1 and -3 expression in lung epithelial cells and promotes allergic airway inflammation. Am J Physiol Lung Cell Mol Physiol 2010;298: L290–L296.
- 45. Yamada N, Yamaya M, Okinaga S, Nakayama K, Sekizawa K, Shibahara S, Sasaki H. Microsatellite polymorphism in the heme oxygenase-1 gene promoter is associated with susceptibility to emphysema. Am J Hum Genet 2000;66:187–195.
- 46. Raval CM, Lee PJ. Heme oxygenase-1 in lung disease. *Curr Drug Targets* 2010;11:1532–1540.
- Nie J, Pei D. Rapid inactivation of alpha-1-proteinase inhibitor by neutrophil specific leukolysin/membrane-type matrix metalloproteinase 6. Exp Cell Res 2004;296:145–150.
- Sozo F, Hooper SB, Wallace MJ. Thrombospondin-1 expression and localization in the developing ovine lung. J Physiol 2007;584:625–635.
- Zhao Y, Xiong Z, Lechner EJ, Klenotic PA, Hamburg BJ, Hulver M, Khare A, Oriss T, Mangalmurti N, Chan Y, et al. Thrombospondin-1 triggers macrophage il-10 production and promotes resolution of experimental lung injury. *Mucosal Immunol* 2014;7:440–448.
- 50. Wurfel MM, Gordon AC, Holden TD, Radella F, Strout J, Kajikawa O, Ruzinski JT, Rona G, Black RA, Stratton S, et al. Toll-like receptor 1 polymorphisms affect innate immune responses and outcomes in sepsis. Am J Respir Crit Care Med 2008;178:710–720.
- 51. Thompson CM, Holden TD, Rona G, Laxmanan B, Black RA, O'Keefe GE, Wurfel MM. Toll-like receptor 1 polymorphisms and associated outcomes in sepsis after traumatic injury: a candidate gene association study. *Ann Surg* 2014;259:179–185.
- 52. Blohmke CJ, Park J, Hirschfeld AF, Victor RE, Schneiderman J, Stefanowicz D, Chilvers MA, Durie PR, Corey M, Zielenski J, et al. TLR5 as an anti-inflammatory target and modifier gene in cystic fibrosis. J Immunol 2010;185:7731–7738.
- 53. Lee CG, Dela Cruz CS, Ma B, Ahangari F, Zhou Y, Halaban R, Sznol M, Elias JA. Chitinase-like proteins in lung injury, repair, and metastasis. *Proc Am Thorac Soc* 2012;9:57–61.
- 54. Ortega H, Prazma C, Suruki RY, Li H, Anderson WH. Association of CHI3L1 in African-Americans with prior history of asthma exacerbations and stress. *J Asthma* 2013;50:7–13.
- 55. Kim YS, Choi SJ, Choi JP, Jeon SG, Oh S, Lee BJ, Gho YS, Lee CG, Zhu Z, Elias JA, et al. IL-12-STAT4-IFN-gamma axis is a key downstream pathway in the development of IL-13-mediated asthma phenotypes in a Th2 type asthma model. Exp Mol Med 2010;42:533–546.
- Yoshida M, Watson RM, Rerecich T, O'Byrne PM. Different profiles of T-cell IFN-gamma and IL-12 in allergen-induced early and dual responders with asthma. J Allergy Clin Immunol 2005;115:1004–1009.

- 57. Shu W, Lu MM, Zhang Y, Tucker PW, Zhou D, Morrisey EE. Foxp2 and Foxp1 cooperatively regulate lung and esophagus development. Development 2007:134:1991–2000.
- 58. Collison A, Hatchwell L, Verrills N, Wark PA, de Siqueira AP, Tooze M, Carpenter H, Don AS, Morris JC, Zimmermann N, et al. The E3 ubiquitin ligase midline 1 promotes allergen and rhinovirus-induced asthma by inhibiting protein phosphatase 2A activity. Nat Med 2013; 19:232–237.
- 59. Wang Y, Wimmer U, Lichtlen P, Inderbitzin D, Stieger B, Meier PJ, Hunziker L, Stallmach T, Forrer R, Rulicke T, et al. Metal-responsive transcription factor-1 (MTF-1) is essential for embryonic liver development and heavy metal detoxification in the adult liver. FASEB J 2004;18:1071–1079.
- Chang DR, Martinez Alanis D, Miller RK, Ji H, Akiyama H, McCrea PD, Chen J. Lung epithelial branching program antagonizes alveolar differentiation. *Proc Natl Acad Sci USA* 2013;110: 18042–18051.
- 61. Hersh CP, Silverman EK, Gascon J, Bhattacharya S, Klanderman BJ, Litonjua AA, Lefebvre V, Sparrow D, Reilly JJ, Anderson WH, et al. SOX5 is a candidate gene for chronic obstructive pulmonary disease susceptibility and is necessary for lung development. Am J Respir Crit Care Med 2011;183:1482–1489.
- 62. Gronostajski RM. Roles of the NFI/CTF gene family in transcription and development. *Gene* 2000;249:31–45.
- 63. Teves ME, Zhang Z, Costanzo RM, Henderson SC, Corwin FD, Zweit J, Sundaresan G, Subler M, Salloum FN, Rubin BK, et al. Sperm-associated antigen-17 gene is essential for motile cilia function and neonatal survival. Am J Respir Cell Mol Biol 2013;48: 765–772.
- 64. Cruciat CM, Dolde C, de Groot RE, Ohkawara B, Reinhard C, Korswagen HC, Niehrs C. RNA helicase DDX3 is a regulatory subunit of casein kinase 1 in Wnt-beta-catenin signaling. *Science* 2013;339: 1436–1441.
- Klinger S, Turgeon B, Levesque K, Wood GA, Aagaard-Tillery KM, Meloche S. Loss of ERK3 function in mice leads to intrauterine growth restriction, pulmonary immaturity, and neonatal lethality. *Proc Natl Acad Sci USA* 2009;106:16710–16715.
- 66. Kramer EL, Hardie WD, Mushaben EM, Acciani TH, Pastura PA, Korfhagen TR, Hershey GK, Whitsett JA, Le Cras TD. Rapamycin decreases airway remodeling and hyperreactivity in a transgenic model of noninflammatory lung disease. *J Appl Physiol* 1985;2011: 1760–1767.
- 67. Mozaffarian A, Brewer AW, Trueblood ES, Luzina IG, Todd NW, Atamas SP, Arnett HA. Mechanisms of oncostatin M-induced pulmonary inflammation and fibrosis. *J Immunol* 2008;181:7243–7253.
- Nogueira-Silva C, Piairo P, Carvalho-Dias E, Veiga C, Moura RS, Correia-Pinto J. The role of glycoprotein 130 family of cytokines in fetal rat lung development. *PLoS ONE* 2013;8:e67607.
- 69. Kormann MS, Depner M, Hartl D, Klopp N, Illig T, Adamski J, Vogelberg C, Weiland SK, von Mutius E, Kabesch M. Toll-like receptor heterodimer variants protect from childhood asthma. *J Allergy Clin Immunol* 2008;122:86–92.
- Kesimer M, Ehre C, Burns KA, Davis CW, Sheehan JK, Pickles RJ. Molecular organization of the mucins and glycocalyx underlying mucus transport over mucosal surfaces of the airways. *Mucosal Immunol* 2013;6:379–392.
- 71. Leikauf GD, Borchers MT, Prows DR, Simpson LG. Mucin apoprotein expression in COPD. *Chest* 2002;121:166S–182S.
- Shi W, Chen H, Sun J, Chen C, Zhao J, Wang YL, Anderson KD, Warburton D. Overexpression of Smurf1 negatively regulates mouse embryonic lung branching morphogenesis by specifically reducing Smad1 and Smad5 proteins. Am J Physiol Lung Cell Mol Physiol 2004;286:L293–L300.
- 73. Xu B, Chen C, Chen H, Zheng SG, Bringas P Jr, Xu M, Zhou X, Chen D, Umans L, Zwijsen A, et al. Smad1 and its target gene Wif1 coordinate BMP and Wnt signaling activities to regulate fetal lung development. Development 2011;138:925–935.
- Taylor BK, Stoops TD, Everett AD. Protein phosphatase inhibitors arrest cell cycle and reduce branching morphogenesis in fetal rat lung cultures. Am J Physiol Lung Cell Mol Physiol 2000;278: L1062–L1070.

- Kobayashi Y, Mercado N, Barnes PJ, Ito K. Defects of protein phosphatase 2A causes corticosteroid insensitivity in severe asthma. PLoS ONE 2011:6:e27627.
- Kaarteenaho R, Merikallio H, Lehtonen S, Harju T, Soini Y. Divergent expression of claudin -1, -3, -4, -5 and -7 in developing human lung. Respir Res 2010:11:59.
- 77. Jang AS, Concel VJ, Bein K, Brant KA, Liu S, Pope-Varsalona H, Dopico RA Jr, Di YP, Knoell DL, Barchowsky A, et al. Endothelial dysfunction and claudin 5 regulation during acrolein-induced lung injury. Am J Respir Cell Mol Biol 2011;44:483–490.
- Ohta H, Chiba S, Ebina M, Furuse M, Nukiwa T. Altered expression of tight junction molecules in alveolar septa in lung injury and fibrosis. Am J Physiol Lung Cell Mol Physiol 2012;302:L193–L205.
- Tao T, Lan J, Presley JF, Sweezey NB, Kaplan F. Nucleocytoplasmic shuttling of Igl2 is developmentally regulated in fetal lung. Am J Respir Cell Mol Biol 2004;30:350–359.
- Diez-Roux G, Banfi S, Sultan M, Geffers L, Anand S, Rozado D, Magen A, Canidio E, Pagani M, Peluso I, et al. A high-resolution anatomical atlas of the transcriptome in the mouse embryo. PLoS Biol 2011;9: e1000582.
- Morrisey EE, Hogan BL. Preparing for the first breath: genetic and cellular mechanisms in lung development. *Dev Cell* 2010;18: 8–23
- Lavoie PM, Pham C, Jang KL. Heritability of bronchopulmonary dysplasia, defined according to the consensus statement of the national institutes of health. *Pediatrics* 2008;122:479–485.
- Gough A, Linden M, Spence D, Patterson CC, Halliday HL, McGarvey LP. Impaired lung function and health status in adult survivors of bronchopulmonary dysplasia. *Eur Respir J* 2014;43:808–816.
- Massaro D, Massaro GD. Critical period for alveologenesis and early determinants of adult pulmonary disease. Am J Physiol Lung Cell Mol Physiol 2004;287:L715–L717.
- 85. Martinez FD. The origins of asthma and chronic obstructive pulmonary disease in early life. *Proc Am Thorac Soc* 2009;6:272–277.
- Svanes C, Sunyer J, Plana E, Dharmage S, Heinrich J, Jarvis D, de Marco R, Norback D, Raherison C, Villani S, et al. Early life origins of chronic obstructive pulmonary disease. *Thorax* 2010; 65:14–20.
- Stocks J, Sonnappa S. Early life influences on the development of chronic obstructive pulmonary disease. Ther Adv Respir Dis 2013;7:161–173.
- Shi W, Bellusci S, Warburton D. Lung development and adult lung diseases. Chest 2007;132:651–656.
- Warburton D, Schwarz M, Tefft D, Flores-Delgado G, Anderson KD, Cardoso WV. The molecular basis of lung morphogenesis. *Mech Dev* 2000;92:55–81.
- Warburton D, Bellusci S, Del Moral PM, Kaartinen V, Lee M, Tefft D, Shi W. Growth factor signaling in lung morphogenetic centers: automaticity, stereotypy and symmetry. Respir Res 2003;4:5.
- 91. Warburton D, Bellusci S, De Langhe S, Del Moral PM, Fleury V, Mailleux A, Tefft D, Unbekandt M, Wang K, Shi W. Molecular mechanisms of early lung specification and branching morphogenesis. *Pediatr Res* 2005;57:26R–37R.
- 92. Shi W, Xu J, Warburton D. Development, repair and fibrosis: what is common and why it matters. *Respirology* 2009;14:656–665.
- 93. Mitzner W. Use of mean airspace chord length to assess emphysema. *J Appl Physiol* 2008;105:1980–1981.
- Giacopelli F, Marciano R, Pistorio A, Catarsi P, Canini S, Karsenty G, Ravazzolo R. Polymorphisms in the osteopontin promoter affect its transcriptional activity. *Physiol Genomics* 2004;20:87–96.
- 95. Schultz J, Lorenz P, Ibrahim SM, Kundt G, Gross G, Kunz M. The functional -443T/C osteopontin promoter polymorphism influences osteopontin gene expression in melanoma cells via binding of c-Myb transcription factor. *Mol Carcinog* 2009;48:14–23.
- 96. D'Alfonso S, Barizzone N, Giordano M, Chiocchetti A, Magnani C, Castelli L, Indelicato M, Giacopelli F, Marchini M, Scorza R, et al. Two single-nucleotide polymorphisms in the 5' and 3' ends of the osteopontin gene contribute to susceptibility to systemic lupus erythematosus. Arthritis Rheum 2005;52:539–547.
- Kariuki SN, Moore JG, Kirou KA, Crow MK, Utset TO, Niewold TB. Age- and gender-specific modulation of serum osteopontin and interferon-alpha by osteopontin genotype in systemic lupus erythematosus. *Genes Immun* 2009;10:487–494.

- Barizzone N, Marchini M, Cappiello F, Chiocchetti A, Orilieri E, Ferrante D, Corrado L, Mellone S, Scorza R, Dianzani U, et al. Association of osteopontin regulatory polymorphisms with systemic sclerosis. Hum Immunol 2011;72:930–934.
- 99. Glas J, Seiderer J, Bayrle C, Wetzke M, Fries C, Tillack C, Olszak T, Beigel F, Steib C, Friedrich M, et al. The role of osteopontin (OPN/SPP1) haplotypes in the susceptibility to Crohn's disease. PLoS ONE 2011;6:e29309.
- 100. Gazal S, Sacre K, Allanore Y, Teruel M, Goodall AH. (The CARDIOGENICS consortium), Tohma S, Alfredsson L, Okada Y, Xie G, Constantin A, Balsa A, Kawasaki A, Nicaise P, Amos C, Rodriguez-Rodriguez L, et al. Identification of secreted phosphoprotein 1 gene as a new rheumatoid arthritis susceptibility gene. Ann Rheum Dis (In press)
- Zhang Z, Deepak V, Meng L, Wang L, Li Y, Jiang Q, Zeng X, Liu W. Analysis of HDAC1-mediated regulation of Runx2-induced osteopontin gene expression in C3h10t1/2 cells. *Biotechnol Lett* 2012;34:197–203.
- 102. Hollingsworth JW, Maruoka S, Boon K, Garantziotis S, Li Z, Tomfohr J, Bailey N, Potts EN, Whitehead G, Brass DM, et al. In utero supplementation with methyl donors enhances allergic airway disease in mice. J Clin Invest 2008;118:3462–3469.
- 103. Haley KJ, Lasky-Su J, Manoli SE, Smith LA, Shahsafaei A, Weiss ST, Tantisira K. RUNX transcription factors: association with pediatric asthma and modulated by maternal smoking. Am J Physiol Lung Cell Mol Physiol 2011;301:L693–L701.
- 104. Srisuma S, Bhattacharya S, Simon DM, Solleti SK, Tyagi S, Starcher B, Mariani TJ. Fibroblast growth factor receptors control epithelial-mesenchymal interactions necessary for alveolar elastogenesis. Am J Respir Crit Care Med 2010;181:838–850.
- 105. Powell-Braxton L, Hollingshead P, Warburton C, Dowd M, Pitts-Meek S, Dalton D, Gillett N, Stewart TA. IGF-I is required for normal embryonic growth in mice. *Genes Dev* 1993;7:2609–2617.
- 106. Briscoe J, Therond PP. The mechanisms of hedgehog signalling and its roles in development and disease. Nat Rev Mol Cell Biol 2013; 14:416–429.
- 107. Chuang PT, Kawcak T, McMahon AP. Feedback control of mammalian Hedgehog signaling by the Hedgehog-binding protein, Hip1, modulates Fgf signaling during branching morphogenesis of the lung. Genes Dev 2003;17:342–347.

- 108. Kerkhof M, Boezen HM, Granell R, Wijga AH, Brunekreef B, Smit HA, de Jongste JC, Thijs C, Mommers M, Penders J, et al. Transient early wheeze and lung function in early childhood associated with chronic obstructive pulmonary disease genes. J Allergy Clin Immunol 2014;133:68–76.
- 109. Pillai SG, Ge D, Zhu G, Kong X, Shianna KV, Need AC, Feng S, Hersh CP, Bakke P, Gulsvik A, et al. A genome-wide association study in chronic obstructive pulmonary disease (COPD): identification of two major susceptibility loci. PLoS Genet 2009; 5:e1000421.
- 110. Zhou X, Baron RM, Hardin M, Cho MH, Zielinski J, Hawrylkiewicz I, Sliwinski P, Hersh CP, Mancini JD, Lu K, et al. Identification of a chronic obstructive pulmonary disease genetic determinant that regulates HHIP. Hum Mol Genet 2012;21: 1325–1335.
- 111. Lamontagne M, Couture C, Postma DS, Timens W, Sin DD, Pare PD, Hogg JC, Nickle D, Laviolette M, Bosse Y. Refining susceptibility loci of chronic obstructive pulmonary disease with lung eqtls. PLoS ONE 2013;8:e70220.
- 112. Li C, Xiao J, Hormi K, Borok Z, Minoo P. Wnt5a participates in distal lung morphogenesis. *Dev Biol* 2002;248:68–81.
- 113. Li C, Hu L, Xiao J, Chen H, Li JT, Bellusci S, Delanghe S, Minoo P. Wnt5a regulates Shh and Fgf10 signaling during lung development. Dev Biol 2005;287:86–97.
- 114. Collins BJ, Kleeberger W, Ball DW. Notch in lung development and lung cancer. Semin Cancer Biol 2004;14:357–364.
- Rock JR, Gao X, Xue Y, Randell SH, Kong YY, Hogan BL. Notchdependent differentiation of adult airway basal stem cells. *Cell Stem Cell* 2011;8:639–664.
- 116. Guseh JS, Bores SA, Stanger BZ, Zhou Q, Anderson WJ, Melton DA, Rajagopal J. Notch signaling promotes airway mucous metaplasia and inhibits alveolar development. *Development* 2009;136: 1751–1759.
- 117. Tsao PN, Vasconcelos M, Izvolsky KI, Qian J, Lu J, Cardoso WV. Notch signaling controls the balance of ciliated and secretory cell fates in developing airways. *Development* 2009;136: 2297–2307.